Journal of Cellular Physiology

Role of NRF2 in preventing oxidative stress induced chloriede current alteration in human lung cells

Journal:	*Journal of Cellular Physiology*
Manuscript ID	JCP-17-0964
Wiley - Manuscript type:	Original Research Article
Date Submitted by the Author:	12-Oct-2017
Complete List of Authors:	Canella, Rita; Università di Ferrara, Dipartimento di Scienze della Vita e Biotecnologie Benedusi, Mascia; Università di Ferrara, Dipartimento di Scienze della Vita e Biotecnologie Martini, Marta; Università di Ferrara, Dipartimento di Scienze della Vita e Biotecnologie Cervellati, Franco; Università di Ferrara, Dipartimento di Scienze della Vita e Biotecnologie Cavicchio, Carlotta; Università di Ferrara, Dipartimento di Scienze della Vita e Biotecnologie Valacchi, Giuseppe; Università di Ferrara, Dipartimento di Scienze della Vita e Biotecnologie
Key Words:	catalase, redox imbalance, ozone, respiratory tract

ROLE OF NRF2 IN PREVENTING OXIDATIVE STRESS INDUCED CHLORIDE CURRENT ALTERATION IN HUMAN LUNG CELLS

Rita Canella[1], Mascia Benedusi[1], Marta Martini[1], Franco Cervellati[1], Carlotta Cavicchio[1] and Giuseppe Valacchi[1-2*]

[1]*Department of Life Sciences and Biotechnology, University of Ferrara, Ferrara, Italy*

[2] *NC State University, Plants for Human Health Institute, Animal Science Dept. NC Research Campus 600 Laureate Way, Kannapolis, NC 28081*

*Corresponding Author

Prof. Giuseppe Valacchi

gvalacc@ncsu.edu

Abstract

The lung tissue is one of the main targets of oxidative stress due to external sources and respiratory activity. In our previous work we have demonstrated in that O_3 exposure alters the Cl^- current-voltage relationship, with the appearance of a large outward rectifier component mainly sustained by ORCCs (Outward Rectifier Chloride Channel) in human lung epithelial cells (A549 line). In the present study we have performed patch clamp experiments, in order to identify which one of the O_3 byproducts (4HNE and/or H_2O_2) was responsible for chloride current change. While 4HNE exposition (up to 25µM for 1h before electrophysiological analysis) did not reproduce O_3 effect, H_2O_2 produced by Glucose Oxidase 10mU for 24h before electrophysiological analysis, mimicked O_3 response. This result was confirmed treating the cell with catalase (CAT) before O_3 exposure (1000 U/ml for 2h): CAT was able to rescue Cl^- current alteration.

Since CAT is regulated by Nrf2 transcription factor, we pre-treated the cells with the Nrf2 activators, Resveratrol and tBHQ. Immunochemical and immunocytochemical results showed Nrf2 activation with both substances that lead to prevent OS effect on Cl^- current.

These data bring new insights on the mechanisms involved in OS induced lung tissue damage by OS, pointing out the role of H_2O_2 in chloride current alteration and the ability of Nfr2 activation in preventing this effect.

INTRODUCTION

Urban pollution is of main public health concern as it affects every living organism on Earth. It has been reported that about 80% of the world's population breathe continuously air whose pollution levels are considered by the World Health Organization extremely dangerous to health. (**OECD, 2011).**

This trend is also true in Europe, as a recent report by the EU commission noted that 9 out of 10 city dwellers are exposed to highly polluted air (**http://www.eea.europa.eu/themes/air/air-pollution-country-fact-sheets-2014)**

The pollution impact will be amplified further in the future by the urbanization megatrend, since 70% of the world's population is expected to be urban by 2050 (**Wilson, 2012**).

As well known, atmospheric pollution is an environmental phenomenon due to the presence into the air of different elements, among which the most toxic are particulate matters, cigarette smoke and ozone (**Bernstain et al., 2004**).

Lung apparatus, being one of the main target of the outdoor stressors, is one of the organs most damaged by air pollution. It is indeed known that breathing polluted air favors the development of pathologies such as asthma, emphysema, chronic obstructive pulmonary disease and also lung cancer **(Ling and van Eeden, 2009; Lopez-Campos et al., 2016)**. In the present work, we have focuses on the harmful effects of tropospheric ozone (O_3) on the lung epithelium. This gas is a widespread secondary pollutant formed by photochemical reactions between nitrogen oxides and volatile organic compounds. Exposure of respiratory epithelial cells to high concentrations of O_3 causes significant damage throughout the whole respiratory tract, however the deepest airways such as bronchioles and alveolar region seem to be the most affected **(Harkema et al., 1987, Stenfors et al., 2002).**

The main toxicological effects associated with O_3 inhalation, include decreased lung function, inflammation of the airways, defective defense mechanisms, higher incidence of respiratory infections and increase and worsening of lung disease (**Ciencewicki et al., 2008**). Ozone causes cell damage by production of reactive oxygen species (ROS) (**Cross et al., 2002)**. These compounds comprise a wide variety of highly reactive metabolites derived from molecular oxygen such as superoxide anion, hydrogen peroxide, and hydroxyl radical and are responsible for numerous and serious damages to DNA, lipids and proteins (**Pryor et al., 1991**). However, cells are able to prevent the accumulation of ROS by maintaining a proper balance between their formation and elimination. These mechanisms include non-enzymatic molecules such as glutathione, vitamins A, C and E and flavonoids in addition to enzymatic

systems such as superoxide dismutase (SOD), catalase (CAT) and glutathione peroxidase (GPx). When the antioxidant capacity of the cell cannot neutralize the excessive production of reactive oxygen species, it is subjected to oxidative stress (**Halliwell and Gutteridge, 2007**). In the lungs, in particular, O_3 reacts with the Epithelial lung Lining Fluid (ELF) producing several byproducts, specially hydrogen peroxide and 4-hydroxynonenale (4HNE), able to promote oxidative damage (**Widdicombe and Widdicombe, 1995; Frampton MW et al., 1999**). Both, H_2O_2 and 4HNE has been shown to stimulate the endogenous cellular defensive system by the activation of (Nuclear erythroid-related factor 2) Nrf2 pathway (**Pecorelli et al., 2013**). The Keap1-Nrf2-ARE pathway plays a crucial role in protecting cells against stress conditions caused by endogenous or exogenous agents (**Kwak et al., 2004**). Under inactivity, the Keap1 protein, predominantly localized in the cytoplasm, binds the Nrf2 transcription factor lowering its half-life to only 20 minutes (**Itoh et al., 1999b**; **McMahon et al., 2003**; **Loboda et al. , 2016**). When, on the other hand, cellular stimuli of oxidative nature occur, Keap1 undergoes modifications leading to the release of Nrf2 and its stabilization with up to 200 minutes half-life (**Ahmed et al** ., 2017) so that, Nrf2 can rapidly move into the nucleus where it binds to the DNA ARE sequences, causing an increase in the transcription of genes encoding for antioxidant enzymes (**Talalay et al., 2003**). At today many compounds have been shown to activate Nrf2, among them Resveratrol and Tert-butylhydroquinone, have been shown to be the best induce of this cellular pathway (**Pervaiz, 2003; Pokorny et al., 2001**). Lung activation of Nrf2 has been involved also in the protection of the respiratory tract against pollution oxidative damage (**Ciencewicki et al., 2008)**.

Injury to type II pneumocytes, the only cells secreting ELF, can alter the whole defensive mechanism of the airways against environmental stressors (**Akella and Deshpande, 2013**). ELF secretion is a delicate process that requires the integrity of the cell membrane ion channels (**Shabbir et al., 2013**). Epithelial chloride channels play a key role in regulating the surfactant ionic composition by controlling the movements of Cl^-, one of main extracellular fluid ion (**Cuppoletti et al., 2000**). Type II cells have different chloride channel classes, among which ORCC (Outward Rectifier Chloride Channel) have been shown to be mainly involved in oxidative stress cellular response (**Canella et al., 2017**). ORCCs are widespread in the body (**Martins et al., 2011**) and their ability to be activated under oxidative stress has been well documented (**Shimizu et al., 2004**).

Therefore, in this paper, after the identification of hydrogen peroxide as the main byproduct of ozone induced chloride channel alteration, we demonstrated the ability of CAT exogenously administrated or induced by RSV and tBHQ through the Keap1-Nrf2-ARE

pathway, to protect the chloride channel functionality when exposed to ozone. In addition, it has now demonstrated that redox cellular homeostasis is maintained by the cross-talk between Nrf2 and NF-kB (**Buelna-Chontal and Zazueta 2013**), for this reason in the present work, also the involvement of NF-kB activation under the proposed experimental conditions has been evaluated.

MATERIALS AND METHODS

Cell culture and treatments

The A-549 (A549: ATCC; Manassas, VA) was cultured in Dulbecco's modified Eagle medium high glucose (DMEM, Lonza®, Milan, Italy) supplemented with 10% fetal bovine serum (FBS, EuroClone, Milan, Italy), L-glutamine at 1% (Lonza, Milan, Italy) and antibiotics Penicillin (100 U / ml) and Streptomycin (100 µg / ml) at 1% (Lonza, Milan, Italy). The cells were then kept in an incubator at a temperature of 37 ° C with 95% humidity and 5% CO_2 until the ideal confluence was reached as previously described **(Valacchi et al., 2011).** A549 cells were treated with 4-hydroxy-2-nonenal (4HNE, 25 µM for 30'; Calbiochem, LaJolla, CA), glucose oxidase (GO, 10 U/ml for 24h; type II from Aspergillus niger,15.5 U/g; Calbiochem, La Jolla, CA) or pretreated with PEG-catalase (PEG-CAT, 1000 U/ml for 2h; SIGMA) or resveratrol (10 µM for 24h; SIGMA) or tert-butylhydroquinone (tBHQ, 10 µM for 24h; SIGMA) before O_3 exposure.

Exposure to Ozone

The cells were exposed to ozone at a concentration of 0.1 ppm for 30 minutes at 37 ° C. Briefly, O_3 was obtained by O_2 subjected to an electric discharge (Ozonizer International Model ECO3, CUV-01, Turin, Italy) and allowed to flow into the teflon coated exposure chamber at a constantly monitored concentration by a specific O_3 detector. Temperature and humidity are also monitored (37 ° C and 45-55% respectively). The O_3 dose and the exposure time were determined by the current literature on O_3 pollution levels and on our recent publications (**Valacchi et al., 2015**).

Resveratrol and tBHQ treatments

For both, resveratrol (RSV) (SIGMA, Milan Italy) and tBQH (SIGMA, Milan Italy), cytotoxicity curve, ranging from 0.1 µM to 50 µM, was performed.
RSV was dissolved in absolute EtOH to obtain a 10 mM stock-solution and tBHQ was prepared in DMSO to obtain a 100 mM stock-solution. Based on the cytotoxicity experiments and the literature **(Plauth et al., 2016; Sticozzi et al., 2014; Takashina et al., 2017; Gharavi et El-Kadi, 2005; Li et al., 2005),** the experiments were performed at 10 µM for both compounds.

Cytotoxicity determination

Cytotoxicity study was performed after the different treatments by measurement of LDH (lactate dehydrogenase) release according to manufacturer's protocol (EuroClone, Milan, Italy). In order to obtain a representative maximal LDH release as the positive control with 100% toxicity, a triplicate set of samples were lysed with 2% (V/V) Triton X-100 in culture media for 30 min at 37 °C.

Nuclear-cytosolic proteins extraction

For cytoplasmic and nuclear extracts, cells were seeded in 100 mm petri (3×10^6 cells). After treatments, cells were detached, washed with ice-cold PBS 1X and cell pellets were resuspended in hypotonic buffer containing 10 mmol/l HEPES (pH 7.9), 10 mmol/l KCl, 1.5 mmol/l MgCl2, 0.3% Nonidet P-40, 0.5 mmol/l dithithreitiol, 0.5 mmol/l phenyl-methyl-sulphonyl fluoride and protease and phosphatase inhibitor cocktails. The lysates were incubated for 15 min on ice and then centrifuged at 1500 × *g* for 5 min at 4 °C for collection of the supernatant containing cytosolic proteins. Supernatants were further centrifuged for 15 min at 24,500 × *g*. Pellets containing the nuclei were resuspended in extraction buffer containing 20 mmol/l HEPES (pH 7.9), 1.5 mmol/l MgCl2, 0.6 mol/l KCl, 0.2 mmol/l EDTA, 20% glycerol, 0.5 mmol/l phenyl-methyl-sulphonyl fluoride and protease and phosphatse inhibitor cocktails, and then incubated for 30 min on ice. Samples were centrifuged at 21,100 × *g* for 15 min to obtain supernatants containing nuclear fractions. Proteins concentration was determined by Bradford analysis (Biorad protein assay; Biorad, Milan, Italy).

Western blot analysis

After protein quantification, 60 μg boiled proteins were loaded into 10% sodium dodecyl sulphate-polycrylamide electrophoresis gels and separated by molecular size. Gels were electro-blotted onto nitrocellulose membranes and then blocked for 90 min in Tris-buffered saline, pH 7.5, containing 0.5% Tween 20 and 5% (w/v) skim milk powder. Membranes were incubated overnight at 4 °C with the appropriate primary antibody: Nrf2 diluted 1:1000 (Millipore, Billerica, Massachusetts) or NF-kB diluted 1:1000 (Millipore, Billerica, Massachusetts). The membranes were finally incubated with the peroxidase-conjugated secondary anti-Rabbit antibody (1:5000) for 1 h. The bound antibodies were detected by chemiluminescence (Biorad, Milan, Italy). β-Actin was used as loading control. Images of the

bands were digitized using an Epson Stylus SX405 scanner and the densitometry analysis was performed using Image-J software.

Immunocytochemistry

A549 cells were grown on coverslips at a density of 1×10^5 cells/ml, and after treatment fixed in 4% paraformaldehyde for 30 min at room temperature (RT). Cells were then permeabilized for 5 min at RT with PBS containing 0.2% Triton X-100, then the coverslips were blocked in PBS containing 1% BSA at RT for 1h. Coverslips were then incubated with primary antibody (1.200) in PBS containing 0.5% BSA at 4°C overnight. After washing, coverslips were incubated with appropriate secondary antibody (1:100) for 1 h at RT. Nuclei were stained with 1 µg/ml DAPI (Sigma- Aldrich) for 1 min. Coverslips were mounted onto glass slides using anti-fade mounting medium 1,4 diazabicyclooctane (DABCO) in glycerine and examined by the Leica light microscope equipped with epifluorescence at × 630 magnification. Negative controls for the immunostaining experiments were performed by omitting primary antibodies. Images were acquired and analyzed with Leica software.

Patch Clamp Technique

Patch pipettes were pulled from glass capillaries with 1.0 mm outer diameter using a micropipette puller (NARISHIGE Instruments, Japan, mod PP-830), fire-polished (tip resistance between 2 and 5 M) and filled with an intracellular solution.

To isolate chloride current intra and extracellular solutions were changed as follows: intracellular solution containing (in mM) 1 MgCl2, 10 HEPES, 5 EGTA and 130 CsCl; pH was adjusted with TEAOH up to the value of 7.4; extracellular solution containing (in mM) 135 NaCl, 1.8 CaCl2, 1 MgCl2, 5.4 KCl, 10 glucose and 10 HEPES; the pH was adjusted with NaOH until the value of 7.35.

Osmolality was adjusted with sucrose to obtain values between 300 and 310 mOsm/Kg. Cells were viewed through a TV monitor connected to a contrast enhanced video camera (T.I.L.L. Photonics, Planegg, Germany). The camera was coupled to an inverted microscope (Olympus IMT-2, Tokyo, Japan) equipped with a 40× Hoffman-modulation contrast objective.

After a gigaseal had been formed, intracellular access was established by suction.

Whole cell currents were elicited by voltage-clamp pulses (1,400 ms duration) between +70 and -110 mV in 20mV increments from a beginning holding potential of -30 mV.

The voltage protocol and data acquisition were performed with Digidata card 1322A and pClamp package (version 9.0). The currents were recorded with a commercial patch clamp

amplifier (EPC-7; Consumer E-List, Darmstadt, Germany); the recordings were filtered at 5 kHz and acquired at 5 (total current) and 10 kHz (chloride current) and stored on disk.

Data analysis and statistical procedures

Data are reported in the text and figures as mean ± SEM. The control-treated comparisons were made with GraphPad Prism v.5, and the significance of P values were reported in the text and figures (two-way ANOVA or one-way ANOVA for set of data; significant differences for $P < 0.05$)

RESULTS

H_2O_2 simulates ozone induced chloride currents

As a follow up of our previous work in which we were able to demonstrate that O_3 exposure is able to alter chloride currents (**Canella et al. 2017**), we want to better understand the byproducts that are responsible for this effect. As mentioned above, since O_3 is too reactive to penetrate the cells, the main byproducts formed by its interaction with the cellular membrane are H_2O_2 and aldehydes, such as 4HNE. Therefore, A549 cells were treated with 4HNE (25 µM for 30') and Glucose Oxidase (GO, 10 U/ml for 24h) to produce H_2O_2, before performing the patch clamp experiments. In Fig.1 it is shown the comparison between current traces of control cell (panel A) and O_3 exposed cell (panel B) respect to the current traces of cells treated with 4HNE or GO (Fig.1 C-D).

It is evident that treatment with 4HNE (panel C) do not affect the time course and the amplitude of currents, while treatment with GO (panel D) seems to replicate the effect of O_3. This result has been confirmed by the I-V curves obtained from the cell samples (4HNE, n=6; GO, n=5) shown in panel E-F. The only curve significantly deviating from control is indeed the one obtained after GO treatment (two-way ANOVA, $P<0.001$).

These data indicate that hydrogen peroxide is able to trigger the increase of the chloride current as observed after O_3 exposure. In order to validate this result, we pre-treated the cells with PEG-catalase (1000 U/ml for 2h), enzyme able to decompose H_2O_2 in oxygen and water, before exposing them to O_3.

Fig.2 shows the comparison between the traces obtained from a control cell (A) and a cell exposed to ozone (B), with those obtained pre-treating the cell with PEG-catalase and then exposing it to O_3 (C). As depicted in the plots, there were no evident changes of amplitude, rising and falling phase between control and the PEG-catalase pre-treated cell. Panel D shows the mean I-V curves obtained from control sample, O_3 exposed sample and PEG-catalase pre-treated sample exposed to O_3 (n=5): the control curve and the PEG-catalase curve are not statistically different (Two-way ANOVA test).

Nrf2 involvement

Based on the results obtained from treating the cells with CAT, we want to further confirm the involvement of H_2O_2 in O_3 induced chloride currents alteration. Therefore, we decided to treat the A549 cells with 2 compounds, resveratrol (RSV) and tert-butylhydroquinone (tBHQ), that can promote endogenous expression of CAT, through the activation of Nrf2, a key transcription factor involved in the activation of the cellular antioxidant defense pathway.

To test whether RSV or tBHQ exert any cytotoxic action on A549 cells, media of samples were collected and lactate dehydrogenase (LDH) release was determined after 24 hours for doses ranging from 0.1 μM to 50 μM for both compounds.

As shown in Fig.3 there was no significant cytotoxicity induced by both RSV (A) and tBHT (B) with all the doses tested (one-way ANOVA).

Based on the results of the cytotoxicity assay, morphological analysis (data not shown) and data in the literature **(Plauth et al., 2016; Sticozzi et al., 2014; Takashina et al., 2017; Gharavi et El-Kadi, 2005; Li et al., 2005)**, the further experiments have been performed at the dose of 10 μM for both compounds.

Therefore, the next step has been to check whether RSV and tBHQ can have an effect on chloride currents. For this purpose, cells were pre-incubated for 24 hours with RSV or tBHQ before patch-clump experiments. In Fig.3C the I-V curves for control cells, RSV (n=7) and tBHQ (n=6) cells are described and it is possible to notice that there was not any significant difference between treated groups and control (Two-way ANOVA test) demonstrating that RSV and tBHQ have no direct effect on the analyzed currents.

Activation of Nrf-2 pathway by Resveratrol and tBHQ

The results in Fig.4B showed that, RSV and tBHQ treatment increases significantly Nrf2 nuclear levels (***), suggesting their ability to induce Nrf2 translocation to the nucleus. This was evidenced by both, immunofluorescence (Fig.4 A-B) and Western blot analysis (Fig. 4C). By the images quantification, it was noticed that nuclear contents of Nrf2 in RSV and tBHQ cells were even higher than the control (###) and O_3 exposed cells (°°°) (one-way ANOVA test *** = $p < 0.001$; ### = $p < 0.001$; °°° = $p < 0.001$).

This indicates that the defensive cellular response is somehow less efficient after O_3 exposure than when the cells are treated with RSV or tBHQ.

Immunochemistry analysis (Fig.4C) confirms the results, with nuclear factor levels higher in tBHQ and RSV treated cells compared to controls and exposed cells (one-way ANOVA test; *** = $p < 0.001$; ### = $p < 0.001$).

Modulation of ozone induced chloride current alteration by RSV and tBHQ treatment

The I-V curves of control cells, ozone exposed cells and Resveratrol pre-treated before ozone expososure(n=6) are described in Fig.5A; while in Fig.5B are depicted the I-V curves of the control group, ozone group and the group pre-treated with tBHQ before being exposed to

ozone (n=5). Two-way ANOVA test between control and pre-treated groups are not significant.

These functional results indicate that both RSV and tBHQ are able prevent the changes in chloride currents induced by ozone.

Effect of resveratrol and tBHQ on NF-kB activation

The pro-inflammatory effect of ozone on lungs has been well demonstrated and recently a cross-talk between Nrf2 and NF-kB has also been suggested. Therefore, we perform experiments aim to evaluate also the involvement of RSV and tBHQ on O_3 induced NF-kB activation.

As shown in Fig.6, immunochemical analysis showed that O_3 was able to clearly induce NF-kB activation (nuclear translocation) respect to the control (One-way ANOVA test; *** = $p < 0.001$). This effect was prevented by the treatment with RSV and tBHQ (One-way ANOVA test; ### = $p < 0.001$) to consolidate indirectly the link between oxidative stress, inflammation and chloride currents.

DISCUSSION

Among the pollutants that are present in the troposphere, ozone is one of the most toxic being formed by the photochemical smog as a consequence of the interaction between UV light and the so called "ozone precursors" nitrogen oxides (NOx), carbon monoxide (CO) and volatile organic compounds (VOCs) (**Bromberg, 2016**). Being a gas, the lung is the main site of ozone effects. Ozone inhalation has been demonstrated to cause airway inflammation in both human and animal studies (**Basha *et al.*, 1994; Devlin *et al.*, 1991, 1996**). The main consequence of a "toxic" ozone exposure can be summarized in airway narrowing, decrements in lung function and epithelial cell barrier function (**Bromberg, 2016**). In a recent paper our group was able to show that ozone is also able to affect chloride current in lung epithelial cells although the mechanism responsible for this effect was not investigated (**Canella et al. 2017**). Ozone is not a radical per se, but it is a very highly reactive oxidant able to react rapidly with C=C double bonds of compounds present in the lung lining fluid (phospholipids, cholesterol and cholesteryl esters) to form a primary ozonide. It has been postulated that O_3 does not react directly with the apical membrane of epithelial cells in conducting airways where the bulk of O_3 uptake takes place since it is not able to penetrate more than about 0.1 μm into the ASL (**Pryor et al., 1991**) although more recently Miller et al. have estimate that most likely ozone is able to penetrate even deeper than 0.1 um, suggesting about 3 μm, which would allow molecular ozone to reach the epithelial surface in bronchioles **(Miller et al., 1985).**

Either by penetrating or by reacting with extracellular molecules it has been clearly shown that ozone is able to react with unsaturated fatty acid residues resulting in the formation of a secondary (Criegee) ozonide and hydroxyhydroperoxide that are the first mediators of ozone "cascade effect" leading to the formation of H_2O_2 e aldheydes. These hydrophilic products, which have been shown to mediate O_3 toxicity.

Therefore, starting from the observation that ozone exposure of A549 cells is able to modulate chloride current (**Canella et al., 2017**), we have first tried to identify whether H_2O_2 and/or 4HNE could be the responsible molecules for ozone effect.

Our investigation identified H_2O_2 as the main chloride current mediator of ozone induced chloride current alteration. Indeed, treating cells with 4HNE did not have any effect on the outward rectifier component (**Bankar et al., 2009**). This result was further confirmed by the administration of catalase to the cells before their exposure to ozone. Catalase is part of the phase II enzymes whose antioxidant function is widely known (**Itoh et al., 1999a**) and it is

able to reduce H_2O_2 in water and oxygen. Pre-treatment of cells with this enzyme, has led to a complete recovery of the function of chloride channel modulated by ozone, bringing current levels to physiological values. This is not the first evidence of the ability of H_2O_2 to alter cellular elettrophysiology, indeed, Filipovic DM and Reeves WB were able to show that H_2O_2 produced a six fold increase in the whole renal cell conductance (**Filipovic et al., 1997**.) suggesting that oxidative stress induced by H_2O_2 can affect cellular electrophysiological status.

Considering the effect of CAT on ozone induced chloride current alteration, we tried to trigger the endogenous antioxidant pathway of the cell, by administrating compounds able to induce the activation of Nrf2, transcription factor that regulates CAT expression **(Talalay et al., 2003)**. Based on the literature, the use of both RSV and tBHQ was investigated (**Satoh et al., 2013, Li et al. 2017**) and our results confirmed their ability to induce Nrf2 activation.

Resveratrol capacity to protect A549 cells against exogenous oxidative stress has been already shown and the results are in line with our work. Indeed, **Kode et al**. (2008) were able to provide evidences that RSV is able to prevent cigarette smoke induced toxicity in the same cellular model by the activation of Nrf2 pathways by restoring GSH cellular depletion. In our case it is more likely that the effect of ozone on chloride channel is linked to CAT activity as the exogenous treatment with peg-CAT was able to restore the physiological chloride currents.

Immunocytochemical and immunochemical analysis have shown that both tBHQ and RSV are able to increase the Nrf2 nucleus translocation in a very effective time and this result would explain why, at a functional level, pre-treatment with both compounds prevents the chloride current from being altered after ozone exposure.

Because cellular homeostasis is tightly regulated by the cross-talk between redox and inflammatory processed of which Nrf2 and NFkB are the main respective players (**Wardyn et al., 2015**), finally we investigated the possible role of RSV and tBHQ in regulating NF-kB (nucleus factor kappa-light-chain-enhancer of B cells) in A549 cells. This protein is involved in the control of the transcription of a wide variety of genes that regulate inflammatory response through the synthesis of cytokines, chemokines, adhesion molecules and other protein compounds (**Van Den Berg et al., 2001**). As observed for Nrf2, also in this case, ozone is responsible for the activation of NF-kB which determines the formation of a dimer, or active protein form (p50 / p65), that migrates into the nucleus, leading to the transcription of target genes involved in the inflammatory process. From the immunochemical analysis emerged that in the cells treated with RSV or tBHQ and eventually exposed to ozone for 30

minutes, the NF-kB nuclear expression levels are lower or comparable to the control condition. This result suggests that tBHQ and RSV may also have a possible anti-inflammatory role that occurs precisely through a reduction in activation and migration of NF-kB into the nucleus. Therefore, the defensive effect could be a consequence of a direct activation of Nrf2 and/or an inhibition of NFkB which negatively regulates Nrf2.

In conclusion these data bring new insights into the mechanisms involved in oxidative stress induced pulmonary tissue damage, highlighting the role of hydrogen peroxide in the alteration of the chloride current and the ability of the cell to modulate membrane currents by means of antioxidant response, by the activation of Nrf2 factor. Moreover, the observed nuclear decrease of NF-kB expression level, suggests that NF-kB activation could be attenuated by different Nrf2 activators. This finding represents an important step to better understand the complex cross-talk between antioxidant and anti-inflammatory pathways in order to ensure cellular homeostasis under oxidative stress conditions and for the first time to our knowledge suggest a redox regulation of chloride channel in lung epithelial cells.

Aknowledgments

The authors declare that there are not any conflict of interests.

REFERENCES

Ahmed SM, Luo L, Namani A, Wang XJ, Tang X. 2017. Nrf2 signaling pathway: Pivotal roles in inflammation. Biochimica et Biophysica Acta (BBA)-Molecular Basis of Disease 1863(2):585-597.

Akella A, Deshpande SB. 2013. Pulmonary surfactants and their role in pathophysiology of lung disorders. Indian J Exp Biol 51:5–22.

Bankar SB, Bule MV, Singhal RS, Ananthanarayan L. 2009. Glucose oxidase--an overview. Biotechnol Adv. 2009 27(4):489-501. doi: 10.1016/j.biotechadv.2009.04.003.

Basha MA, Gross KB, Gwizdala CJ, Haidar AH, Popovich J Jr. 1994. Bronchoalveolar lavage neutrophilia in asthmatic and healthy volunteers after controlled exposure to ozone and filtered purified air. Chest 106(6):1757-65.

Bernstein JA, Alexis N, Barnes C, Bernstein IL, Bernstein JA, Nel A, Peden D, Diaz-Sanchez D, Tarlo SM, Williams PB. 2004. Health effect of air pollution. J Allergy Clin Immunol 114(5):1116-1123.

Bromberg PA. 2016. Mechanisms of the acute effects of inhaled ozone in humans. Biochim Biophys Acta 1860(12):2771-81. doi: 10.1016/j.bbagen.2016.07.015.

Buelna-Chontal M and Zazueta C. 2013. Redox activation of Nrf2 & NF-κB: a double end sword? Cell Signal 25: 2548-57.

Canella R, Martini M, Borriello R, Cavicchio C, Muresan XM, Cervellati F, Valacchi G. 2017. Modulation of chloride currents in human lung epithelial cells exposed to exogenous oxidative stress. J Cell Physiol 232(7):1817-1825. doi: 10.1002/jcp.25705.

Ciencewicki J, Trivedi S, Kleeberger SR. 2008. Oxidants and the pathogenesis of lung diseases. Journal of Allergy and Clinical Immunology 122(3):456-468.

Cross CE, Valacchi G, Schock B, Wilson M, Weber S, Eiserich J, van der Vliet A. 2002. Environmental oxidant pollutant effects on biologic systems: a focus on micronutrient antioxidant-oxidant interactions. Am J Respir Crit Care Med. 166:S44-50.

Cuppoletti J, Teweri KP, Sherry AM, Malinowska DH. 2000. Activation of human ClC-2 Cl-channels: Implications for cystic fibrosis. Clin Exp Pharmacol Physiol 27:896–900.

Devlin RB, McDonnell WF, Mann R, Becker S, House DE, Schreinemachers D, Koren HS. 1991.
Exposure of humans to ambient levels of ozone for 6.6 hours causes cellular and biochemical changes in the lung. Am J Respir Cell Mol Biol 4(1):72-81.

Devlin RB, McDonnell WF, Becker S, Madden MC, McGee MP, Perez R, Hatch G, House DE, Koren HS. 1996. Time-dependent changes of inflammatory mediators in the lungs of humans exposed to 0.4 ppm ozone for 2 hr: a comparison of mediators found in bronchoalveolar lavage fluid 1 and 18 hr after exposure.Toxicol Appl Pharmacol 138(1):176-85.

Filipovic DM, Reeves WB. 1997. Hydrogen peroxide activates glibenclamide-sensitive K+ channels in LLC-PK1 cells. Am J Physiol 272(2 Pt 1):C737-43.

Frampton MW, Pryor WA, Cueto R, Cox C, Morrow PE, Utell MJ. 1999. Ozone exposure increases aldehydes in epithelial lining fluid in human lung. Am J Respir Crit Care Med 159:1134-7.

Gharavi N, El-Kadi AO. 2005. tert-Butylhydroquinone is a novel aryl hydrocarbon receptor ligand.
Drug Metab Dispos 33(3):365-72.

Halliwell B, Gutteridge JMC. 2007. Free Radicals in Biology and Medicine. 4th. Oxford, UK: Clarendon Press

Harkema JR, Plopper CG, Hyde DM, St George JA, Wilson DW, Dungworth DL. 1987. Response of the macaque nasal epithelium to ambient levels of ozone. A morphologic and morphometric study of the transitional and respiratory epithelium. Am J Pathol 128(1):29-44.

Hirose M, Yada H, Hakoi K, Takahashi S, Ito N. 1993. Modification of carcinogenesis by alpha-tocopherol, tbutylhydroquinone, propyl gallate and butylated hydroxytoluene in a rat multi-organ carcinogenesis model. Carcinogenesis 14(11):2359-2364.

Itoh K, Ishii T, Wakabayashi N, Yamamoto M. 1999a. Regulatory mechanisms of cellular response to oxidative stress, Free Radic Res 31:319–324.

Itoh K, Wakabayashi N, Katoh Y, Ishii T, Igarashi K, Engel JD, Yamamoto M. 1999b. Keap1 represses nuclear activation of antioxidant responsive elements by Nrf2 through binding to the amino-terminal Neh2 domain. Genes Dev 13:76–86.

Kode A, Rajendrasozhan S, Caito S, Yang SR, Megson IL, Rahman I. 2008. Resveratrol induces glutathione synthesis by activation of Nrf2 and protects against cigarette smoke-mediated oxidative stress in human lung epithelial cells. Am J Physiol Lung Cell Mol Physiol 294(3):L478-88.

Kwak MK, Wakabayashi N, Kensler TW. 2004. Chemoprevention through the Keap1-Nrf2 signaling pathway by phase 2 enzyme inducers. Mutat Res 555:133–148.

Li B, Hou D, Guo H, Zhou H, Zhang S, Xu X, Liu Q, Zhang X, Zou Y, Gong Y, Shao C. 2017. Resveratrol sequentially induces replication and oxidative stresses to drive p53-CXCR2 mediated cellular senescence in cancer cells. Sci Rep. 7(1):208. doi: 10.1038/s41598-017-00315-4.

Li J, Johnson D, Calkins M, Wright L, Svendsen C, Johnson J. 2005. Stabilization of Nrf2 by tBHQ confers protection against oxidative stress-induced cell death in human neural stem cells. Toxicol Sci 83(2):313-28.

Ling SH, Van Eeden SF. 2009. Particulate matter air pollution exposure: role in the development and exacerbation of chronic obstructive pulmonary disease. Int J Chron Obstruct Pulmon Dis 4:233-243.

Loboda A, Damulewicz M, Pyza E, Jozkowicz A, Dulak J. 2016. Role of Nrf2/HO-1 system in development, oxidative stress response and diseases: an evolutionarily conserved mechanism. Cellular and Molecular Life Sciences 73(17): 3221-3247.

Lopez-Campos JL, Marquez-Martin E, Soriano JB. 2016. The role of air pollution in COPD and implications for therapy. Expert Rev Respir Med 9:1–11.

Martins JR, Faria D, Kongsuphol P, Reisch B, Schreiber R. 2011. Anoctamin 6 is an essential component of the outwardly rectifying chloride channel. PNAS 108:18168–18172.

McMahon M, Itoh K, Yamamoto M, and Hayes JD. 2003. Keap1- dependent proteasomal degradation of transcription factor Nrf2 contributes to the negative regulation of antioxidant response element-driven gene expression. J. Biol. Chem. 278:21592–21600.

Miller FJ, Overton JH Jr, Jaskot RH, Menzel DB. 1985. A model of the regional uptake of gaseous pollutants in the lung. I. The sensitivity of the uptake of ozone in the human lung to lower respiratory tract secretions and exercise. Toxicol Appl Pharmacol 79:11–27

OECD, 2011. OECD Regions at a Glance 2011, OECD Publishing.
http://dx.doi.org/10.1787/reg_glance-2011-en

Pecorelli A, Bocci V, Acquaviva A, Belmonte G, Gardi C, Virgili F, Ciccoli L, Valacchi G. 2013. NRF2 activation is involved in ozonated human serum upregulation of HO-1 in endothelial cells. Toxicol Appl Pharmacol 267:30-40.

Pervaiz S. 2003. Resveratrol: from grapevines to mammalian biology. FASEB J 17:1975–1985.

Plauth A, Geikowski A, Cichon S, Wowro SJ, Liedgens L, Rousseau M, Weidner C, Fuhr L, Kliem M, Jenkins G, Lotito S, Wainwright LJ, Sauer S. 2016. Data of oxygen- and pH-dependent oxidation of resveratrol. Data Brief 9:433-437.

Pokorny J, Yanishlieva N, Gordon M. 2001. Antioxidants in Food: Practical Applications. CRC Press.

Pryor WA, Das B, Church DF. 1991. The ozonation of unsaturated fatty acids: aldehydes and hydrogen peroxide as products and possible mediators of ozone toxicity. Chem Res Toxicol 4(3):341-348.

Satoh T, McKercher SR, Lipton SA. 2013. Nrf2/ARE-mediated antioxidant actions of pro-electrophilic drugs. Free Radic Biol Med 65:645-57. doi: 10.1016/j.freeradbiomed.**2013**.07.022.

Shabbir W, Scherbaum-Hazemi P, Tzotzos S, Fischer B, Fischer H, Pietschmann H, Lucas R, Lemmens-Gruber R. 2013. Mechanism of action of novel lung edema therapeutic AP301 by activation of the epithelial sodium channel. Mol pharmacol 84(6):899-910.

Shimizu T, Numata T, Okada Y. 2004. A role of reactive oxygen species in apoptotic activation of volume-sensitive Cl- channel. Proc Natl Acad Sci USA 101(17):6770-6773.

Stenfors N, Pourazar J, Blomberg A, Krishna MT, Mudway I, Helleday R, Kelly FJ, Frew AJ, Sandström T. 2002. Effect of ozone on bronchial mucosal inflammation in asthmatic and healthy subjects. Respir Med 96: 352-8.

Sticozzi C, Cervellati F, Muresan XM, Cervellati C, Valacchi G. 2014. Resveratrol prevents cigarette smoke-induced keratinocytes damage. Food Funct 5(9):2348-56. doi: 10.1039/c4fo00407h.

Takashina M, Inoue S, Tomihara K, Tomita K, Hattori K, Zhao QL, Suzuki T, Noguchi M, Ohashi W, Hattori Y. 2017. Different effect of resveratrol to induction of apoptosis depending on the type of human cancer cells. Int J Oncol 50(3):787-797. doi: 10.3892/ijo.2017.3859.

Talalay P, Dinkova-Kostova AT, Holtzclaw WD. 2003. Importance of phase 2 gene regulation in protection against electrophile and reactive oxygen toxicity and carcinogenesis. Adv Enzyme Regul 43:121–134.

Valacchi G, Davis PA, Khan EM, Lanir R, Maioli E, Pecorelli A, Cross CE, Goldkorn T. 2011. Cigarette smoke exposure causes changes in Scavenger Receptor B1 level and distribution in lung cells. Int J Biochem Cell Biol 43: 1065-70.

Valacchi G, Sticozzi C, Belmonte G, Cervellati F, Demaude J, Chen N, Krol Y, Oresajo C. 2015. Vitamin C compound mixtures prevent ozone-induced oxidative damage in human keratinocytes as initial assessment of pollution protection. PLoS ONE 10:e0131097.

Van den Berg R, Haenen G, Van den Berg H, Bast A. 2001. Transcription factor NF-κB as a potential biomarker for oxidative stress. British Journal of Nutrition 86(S1): S121-S127.

Wardyn JD, Ponsford AH, Sanderson CM. 2015. Dissecting molecular cross-talk between Nrf2 and NF-κB response pathways. Biochem Soc Trans 43(4):621-6.

Widdicombe JH, Widdicombe JG. 1995. Regulation of human airway liquid. Respir Physiol 99:3–12.

Wilson, M. 2012. Co.Design. Consulté le October 9, 2012, sur FastCompany: http://www.fastcodesign.com/1669244/by-2050-70-of- the-worlds-population-will-be-urban-is-that-a-good-thing

SITOGRAPHY

http://www.eea.europa.eu/themes/air/air-pollution-country-fact-sheets-2014

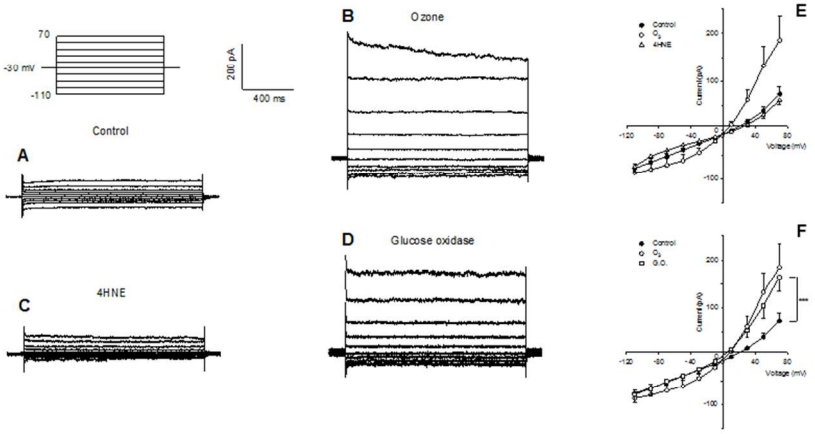

Fig. 1: Representative families of chloride recording currents in control condition (A), after exposure to O3 (B), after 4HNE (C), and GO (D) treatments. Panel E: current-voltage relationship of control (n = 11), exposed to O3 (n = 5) and treated with 4HNE (n = 6) cells. Panel F: current-voltage relationship of control (n = 11), exposed to O3 (n = 5), treated with H2O2 (n = 7) and treated with GO cells (n = 5). The comparison between the control group and the treated groups was not significant; the comparison between control group and GO treated group is very significant (Two-way ANOVA, P < 0.001).

254x190mm (96 x 96 DPI)

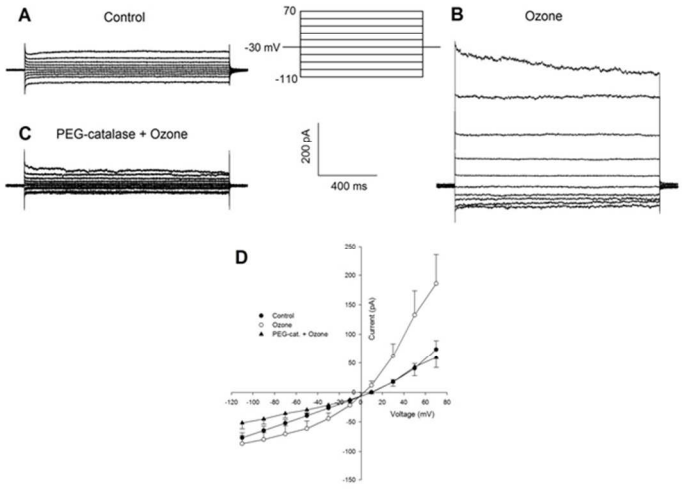

Fig. 2 Panels A, B, C: Examples of current trace recordings obtained from a control cell, a cell exposed to O3 and a cell treated with PEG-catalase and subsequently exposed to Ozone, respectively.
Panel D: Current-voltage curves of control cells (n = 11), cells treated with O3 (n = 5) and cells treated with PEG-Catalase and O3 (n = 5). Comparison between controls and cells treated with PEG-catalase + O3 was performed with two-way ANOVA and was not significant

254x190mm (96 x 96 DPI)

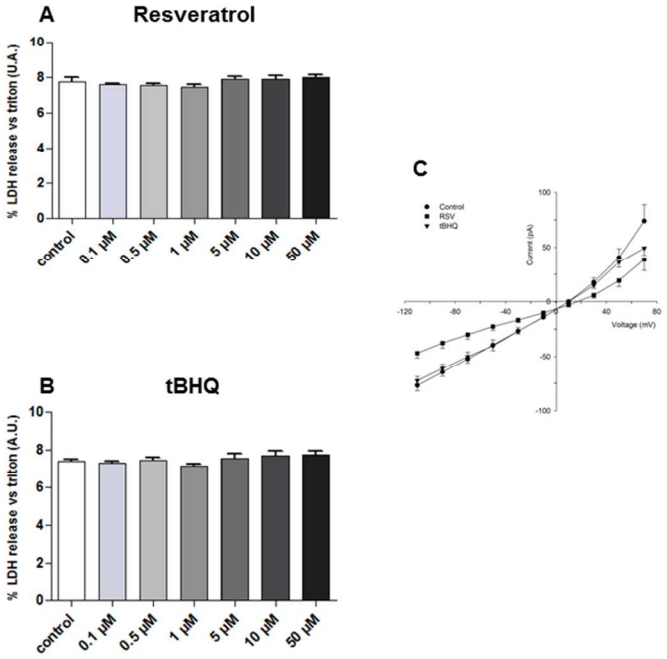

Fig. 3: Cytotoxicity assay of LDH release in A549 cells treated with resveratrol (A) and tBHQ (B) at different doses. Panel C: Current-Voltage relationship of control cells (n = 11) treated with Resveratrol cells (n = 7) and treated with tBHQ (n = 6) cells.

254x190mm (96 x 96 DPI)

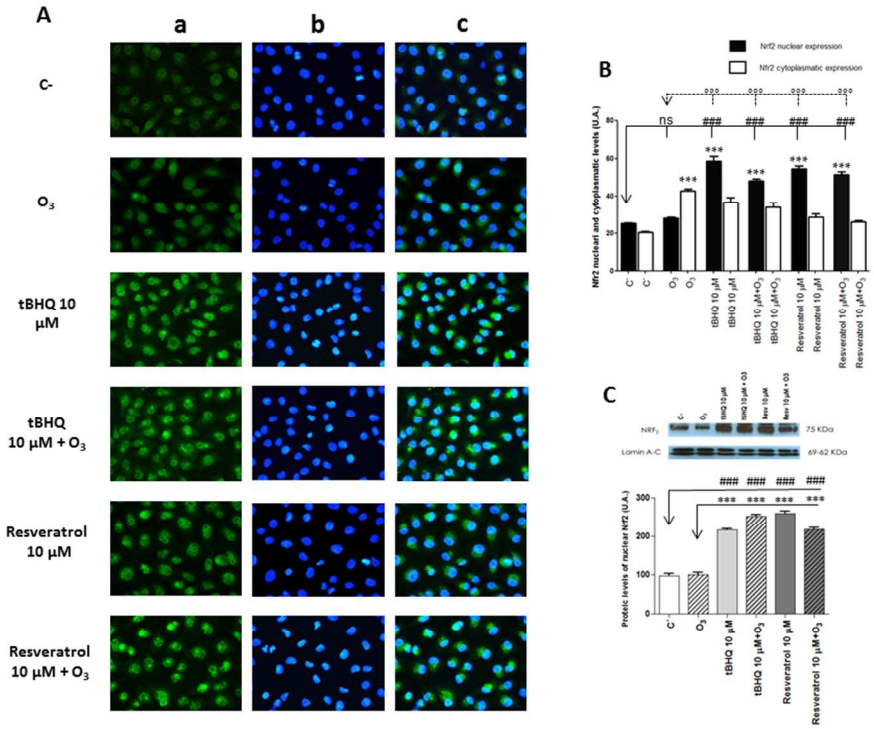

Fig. 4: Representative images of immunocytochemistry for Nrf2 in A-549 cells: (a) fitc 40x, (b) 40x daps, (c) merge 40x under the various experimental conditions. Panel B: Immunocytochemical analysis of Nrf2 nuclear and cytoplasmic expression levels in control group (C-); exposed to O3 group; tBHQ treated group; tBHQ pre-treated and O3 exposed group; RSV treated group; RSV pre-treated and O3 exposed group. Data were normalized with respect to the O3 treated sample and expressed as arbitrary units ± SEM. Panel C: Western blot analysis. Nuclear expression of Nrf2 protein in control group (C-); exposed to O3 group; tBHQ treated group; tBHQ pre-treated and O3 exposed group; RSV treated group; RSV pre-treated and O3 exposed group. Above, a typical Western blot for Nfr2 is shown, with laminin (loading control); below the quantification of the obtained bands are represented; data are expressed as arbitrary units, mean ± SEM. Statistical test one-way-ANOVA.

254x190mm (96 x 96 DPI)

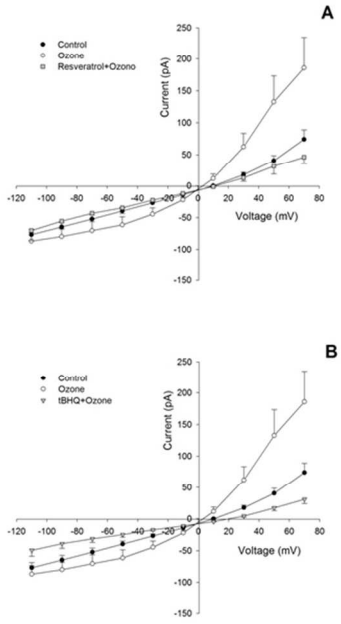

Figure 5: (A) current-voltage curves of control cells (n = 11), exposed to ozone (n = 5) and treated with Resveratrol + O3 (n = 6) cells; (B) current-voltage curves of control cells (n = 11), exposed to ozone (n = 5) and treated with tBHQ + O3 (n = 6). The comparisons between the control group and the treated groups were not significant (Two-way ANOVA).

254x190mm (96 x 96 DPI)

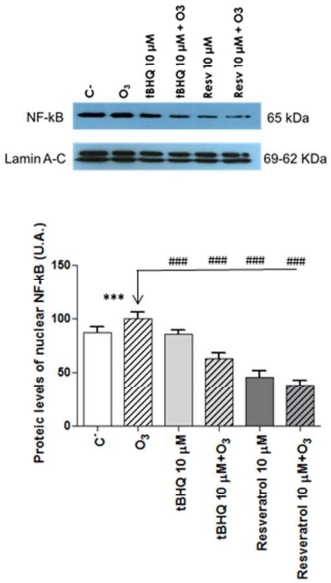

Fig. 6: Nucleic expression of NF-kB protein in A549 cells exposed to O3, treated with tBHQ/Resveratrol, treated with tBHQ/Resveratrol + O3. In the upper panel a typical Western blot for NF-kB is shown, with its loading control. In the lower panel the quantification of the obtained bands is described; data are expressed in arbitrary units as mean ± SEM. Statistical test One-way ANOVA.

254x190mm (96 x 96 DPI)